

mTOR Regulates Gap Junction Alpha-1 Protein Trafficking in Sertoli Cells and Is Required for the Maintenance of Spermatogenesis in Mice¹

Alexandre Boyer,⁴ Meggie Girard,⁴ Dayananda S. Thimmanahalli,^{3,5} Adrien Levasseur,⁴ Christophe Céleste,⁴ Marilène Paquet,⁴ Rajesha Duggavathi,⁵ and Derek Boerboom^{2,4}

⁴Centre de Recherche en Reproduction Animale, Faculté de Médecine Vétérinaire, Université de Montréal, Montréal, Québec, Canada

⁵Department of Animal Science, McGill University, Sainte-Anne-de-Bellevue, Québec, Canada

ABSTRACT

The mammalian target of rapamycin (*Mtor*) gene encodes a serine/threonine kinase that acts as a master regulator of processes as diverse as cell growth, protein synthesis, cytoskeleton reorganization, and cell survival. In the testis, physiological roles for *Mtor* have been proposed in perinatal Sertoli cell proliferation and blood–testis barrier (BTB) remodeling during spermatogenesis, but no *in vivo* studies of *Mtor* function have been reported. Here, we used a conditional knockout approach to target *Mtor* in Sertoli cells. The resulting *Mtor*^{flox/flox}; *Amhr2*^{cre/+} mice were characterized by progressive, adult-onset testicular atrophy associated with disorganization of the seminiferous epithelium, loss of Sertoli cell polarity, increased germ cell apoptosis, premature release of germ cells, decreased epididymal sperm counts, increased sperm abnormalities, and infertility. Histopathologic analysis and quantification of the expression of stage-specific markers showed a specific loss of pachytene spermatocytes and spermatids. Although the BTB and the ectoplasmic specializations did not appear to be altered in *Mtor*^{flox/flox}; *Amhr2*^{cre/+} mice, a dramatic redistribution of gap junction alpha-1 (GJA1) was detected in their Sertoli cells. Phosphorylation of GJA1 at Ser373, which is associated with its internalization, was increased in the testes of *Mtor*^{flox/flox}; *Amhr2*^{cre/+} mice, as was the expression and phosphorylation of AKT, which phosphorylates GJA1 at this site. Together, these results indicate that *Mtor* expression in Sertoli cells is required for the maintenance of spermatogenesis and the progression of germ cell development through the pachytene spermatocyte stage. One mechanism of mTOR action may be to regulate gap

junction dynamics by inhibiting AKT, thereby decreasing GJA1 phosphorylation and internalization. mTOR regulates gap junction alpha-1 protein distribution in Sertoli cells and is necessary for progression through the pachytene spermatocyte stage.

Cre-lox, *GJA1*, *mTOR*, Sertoli cells, spermatogenesis, testicular degeneration

INTRODUCTION

The mammalian target of rapamycin (*Mtor*) gene product is a ubiquitous serine/threonine kinase involved in many aspects of cellular function including cell growth and proliferation [1], cytoskeleton reorganization, motility, cell survival, and autophagy [1–4]. It acts as a master regulator and is able to integrate the inputs of growth factors, hormones, mitogens, and nutrients [1] to ensure appropriate cellular responses to environmental changes. mTOR is the catalytic subunit of two distinct multiprotein complexes: mTORC1 and mTORC2 [1, 5]. The rapamycin-sensitive mTORC1 is composed of mTOR, regulatory-associated protein of mTOR (Raptor), mammalian lethal with SEC13 protein 8 (mLST8), and the noncore proteins proline-rich Akt/protein kinase B (PRAS40), FK506-binding protein 38 (FKBP38), and Rag GTPases, and regulates cell growth and proliferation by modulating protein synthesis. mTORC2 is composed of mTOR, rapamycin-insensitive companion of mTOR (Rictor), mLST8, and mammalian stress-activated protein kinase interacting protein 1 (mSIN1), and regulates the actin cytoskeleton and cell survival [1, 5].

A role for mTORC1 in male reproductive physiology was first proposed when it was shown that rapamycin impairs testicular function in both rodents and humans [6–12]. Male patients treated with analogs of rapamycin have decreased testosterone levels and sperm counts, as well as increased follicle-stimulating hormone and luteinizing hormone levels [7], suggesting inhibition of the hypothalamic–pituitary–gonad axis. Subsequent studies of mTOR signaling in the testis have focused on two cell types, spermatogonial stem cells (SSCs) and Sertoli cells. In SSCs, mTORC1 activity has been shown to inhibit SSC maintenance by inhibiting glial cell line-derived neurotrophic factor (GDNF) signaling, and zinc finger and blood–testis barrier (BTB) domain containing 16 (ZBTB16 [also known as PLZF]) acts to antagonize mTORC1 in this context [13]. Activation of the PI3K/AKT/mTORC1 signaling pathway by retinoic acid leads to the translational activation of mRNAs encoding regulators of SSC differentiation [14, 15]. In addition, conditional deletion of the mTORC1 inhibitor tuberous sclerosis 2 (*Tsc2*) gene in germ cells has been shown to promote the differentiation of SSCs, leading to the loss of the SSC pool and germline degeneration [16]. Together, these

¹Supported by National Sciences and Engineering Research Council Discovery grants to D.B., R.D., and A.B.; Canada Research Chair in Ovarian Molecular Biology and Functional Genomics to D.B.; National Institute of Child Health and Human Development (Specialized Cooperative Centers Program in Reproduction Research) grant U54-HD28934; and University of Virginia Center for Research in Reproduction Ligand Assay and Analysis Core. Presented in part at the 46th Annual Meeting of the Society for the Study of Reproduction, July 22–26, 2013, Montreal, Quebec, Canada.

²Correspondence: Derek Boerboom, Centre de Recherche en Reproduction Animale, Faculté de Médecine Vétérinaire, Université de Montréal, 3200 rue Sicotte, St-Hyacinthe, QC, J2S 7C6, Canada. E-mail: derek.boerbom@umontreal.ca

³Current address: Goodman Cancer Research Centre, McGill University, Montreal, Quebec, Canada.

Received: 18 December 2015.
First decision: 14 February 2016.
Accepted: 17 May 2016.

© 2016 by the Society for the Study of Reproduction, Inc. This article is available under a Creative Commons License 4.0 (Attribution-Non-Commercial), as described at <http://creativecommons.org/licenses/by-nc/4.0>
eISSN: 1529-7268 <http://www.biolreprod.org>
ISSN: 0006-3363

studies indicate that activation of mTORC1 favors the differentiation of SSCs at the expense of their maintenance and proliferation.

Both mTORC1 and mTORC2 have been implicated in Sertoli cell functions. Follicle-stimulating hormone regulates the PI3K/AKT/mTORC1 pathway in cultured proliferating rat Sertoli cells, and it has been proposed that this pathway could be important for the mitotic activity of Sertoli cells during the neonatal period [17, 18]. It was also shown that rapamycin affects Sertoli cell nutritional metabolism and redox state [19]. Recent studies have also focused on the role of mTOR in BTB dynamics during spermatogenesis. Notably, *in vitro* studies have suggested that ribosomal protein S6 (RPS6, a downstream target of mTORC1) and Rictor have opposing effects on BTB restructuring during specific stages of spermatogenesis, with RPS6 promoting opening of the BTB and Rictor its stability [20–23]. Conditional deletion of Rictor in Sertoli cells leads to azoospermia due to the disruption of actin organization in Sertoli cells and their subsequent loss of polarity [24]. Although these studies suggest that mTOR complexes could play critical roles in Sertoli cells, no direct *in vivo* studies of mTOR function have been reported thus far. In the present study, we aimed to elucidate the role of *Mtor* in Sertoli cells by inactivating its expression in a transgenic mouse model.

MATERIALS AND METHODS

Transgenic Mouse Strains

Mtor^{tm1.2Koz/tm1.2Koz};*Amhr2*^{tm3(cre)Bhr/+} mice were derived by crossing mice bearing *Mtor*^{tm1.2Koz} (hereafter *Mtor*^{fllox}) and *Amhr2*^{tm3(cre)Bhr} (hereafter *Amhr2*^{cre/+}) alleles, and genotype analyses were carried out by PCR as previously described [25, 26]. All animal procedures were approved by the Comité d'Éthique de l'Utilisation des Animaux of the Université de Montréal (protocol Rech-1320) and conformed to the International Guiding Principles for Biomedical Research Involving Animals as promulgated by the Society for the Study of Reproduction.

Primary Sertoli Cell Isolation

Sertoli cells from 3-week-old animals were purified as previously described [27]. Briefly, testes were decapsulated, and seminiferous tubules were pooled and washed with phosphate-buffered saline (PBS). The tubules were then incubated with 2 mg/ml collagenase I (Sigma-Aldrich) and 0.5 mg/ml DNase I (Sigma-Aldrich) in Dulbecco modified Eagle medium (DMEM) for 30 min at 37°C on a shaker. The tubules were then washed twice with DMEM and digested further with 2 mg/ml collagenase I, 0.5 mg/ml DNase I, and 1 mg/ml hyaluronidase type III (Sigma-Aldrich) for 20–30 min at 37°C. After settling, the tubules were washed twice with DMEM and digested further with 2 mg/ml collagenase I, 0.5 mg/ml DNase I, 2 mg/ml hyaluronidase, and 1 mg/ml trypsin for 40–60 min at 37°C. The dispersed cells were then washed twice with DMEM and placed into culture dishes in DMEM containing 10% fetal calf serum and incubated at 37°C and 5% CO₂. Hypotonic treatment was applied with 20 mM Tris-HCl, pH 7.4, and medium was changed after the first day to remove germ cells. Attached Sertoli cells (typically 80%–90% pure, as determined by SOX9 cytofluorescence) were then harvested for genotype or reverse transcription-quantitative polymerase chain reaction (RT-qPCR) analyses, as described above and below, respectively.

Sperm Counts and Analyses

Cauda epididymides were placed in prewarmed (37°C) minimum essential medium containing bovine serum albumin (3 mg/ml), and epididymal ducts were opened to release their contents. For sperm count analysis, 500 µl of sperm suspension was pipetted into a tube containing 2 ml of PBS and placed in a water bath for 1 min at 60°C to halt sperm motility and then cooled to room temperature. After being mixed gently, 10 µl of sperm suspension was loaded to each side of a hemocytometer and allowed 2 min for the spermatozoa to settle. Counting was done in duplicate, and total sperm counts were calculated according to guidelines described previously [28].

For evaluation of sperm morphology, 100 µl of sperm suspension was pipetted into 1 ml of 10% neutral buffered formalin containing 1 drop of 5% eosin Y aqueous. After gentle mixing, the suspension was incubated at room

temperature for one hour. From this sperm suspension, smears were prepared by drying and fixation in methanol for 5 min. A total of 1000 spermatozoa were evaluated for each sample, except when low sperm counts prevented this, in which case all spermatozoa present in the smear were evaluated.

Quantitative Reverse Transcription PCR

Total RNA from cultured Sertoli cells and from testes from 3- and 5-mo-old animals was extracted using the RNeasy mini-kit (Qiagen) according to the manufacturer's protocol. Total RNA was reverse transcribed using 100 ng of RNA and the SuperScriptVilo cDNA synthesis kit (Thermo Fisher Scientific). Real-time PCR reactions were run using an ABI Prism 7300 instrument with Power SYBR Green PCR Master Mix (Applied Biosystems). Each PCR reaction consisted of 12.5 µl of Power SYBR Green PCR Master Mix, 9.5 µl of water, 1 µl of cDNA sample, and 1 µl (10 pmol) of gene-specific primer. PCR reactions run without cDNA (water blank) served as negative controls. A common thermal cycling program (3 min at 95°C, 40 cycles of 15 sec at 95°C, 30 sec at 60°C, and 30 sec at 72°C) was used to amplify each transcript. To quantify relative gene expression, the cycle threshold (C_t) values for *Mtor*, DNA meiotic recombinase 1 (*Dmc1*), synaptonemal complex 3 (*Sycp3*), Calmegin (*Clgn*), spermatid associated (*Spert*), and diazepam binding inhibitor like-5 (*Dhil5*) amplification were compared with that of *Rpl19*, according to the ratio $[R = (E^{Ct_{Rpl19}}/E^{Ct_{target}})]$, where *E* is the amplification efficiency for each primer pair. *Rpl19* C_t values did not change significantly between genotypes and treatments, and *Rpl19* was therefore deemed suitable as an internal reference gene. The specific primer sequences used are listed in Supplemental Table S1 (all Supplemental Data are available online at www.biolreprod.org).

Histopathology and Immunohistochemistry

Testes for histopathology analysis by light microscopy were weighed, fixed in Bouin fixative for 24 h, rinsed, and dehydrated in alcohol and subsequently embedded in paraffin, sectioned, and stained using the periodic acid-Schiff and hematoxylin (PAS-H) method. The stage of the spermatogenesis cycle was determined in 50 randomly selected seminiferous tubules per histologic section (n = 6 for mutant and control animals, 1 section per animal) by a veterinary pathologist and based on established morphological criteria [29]. Immunohistochemistry was carried out using Bouin-fixed, paraffin-embedded, 7-µm-thick tissue sections in VectaStain Elite avidin-biotin complex method kits (Vector Laboratories) as directed by the manufacturer. Sections were probed with a primary antibody against GJA1 (1:100 dilution; catalog no. 3512; Cell Signaling), and stained using the 3,3'-diaminobenzidine peroxidase substrate kit (Vector Laboratories).

TUNEL Analysis

Terminal deoxynucleotidyltransferase dUTP nick-end labeling (TUNEL) assay was performed using Bouin-fixed, paraffin-embedded, 7-µm-thick section testis and In Situ Cell Death Detection kit TMR red (Roche) as directed by the manufacturer. Slides were mounted using VectaShield with 4',6-diamidino-2-phenylindole (DAPI; Vector Laboratories).

Immunoprecipitation and Immunoblotting

Protein extracts were prepared from testes using T-Per solution (Pierce) as directed by the manufacturer and stored at –80°C until further analyses. Protein concentrations were determined using the Bradford method (Bio-Rad protein assay; Bio-Rad Laboratories). For immunoprecipitation, 200 µg of protein per sample was diluted in radioimmunoprecipitation assay (RIPA) buffer (400 µl) containing protease inhibitors and precleared for 30 min with 15-µl Dynabeads protein G (Invitrogen) at 4°C. Half of the supernatant was then incubated with 2 µg of rabbit anti-GJA1 (product C6219; Sigma-Aldrich) and the other half with 2 µg of immunoglobulin G (IgG; catalog no. 3900; Cell Signaling) for 60 min at 4°C. Dynabeads (15 µl) were then added for 45 min at 4°C, the beads were washed five times with 1 ml of RIPA buffer, and bound proteins were eluted and denatured by addition of boiling SDS-PAGE sample buffer.

For immunoblotting, immunoprecipitates or protein extracts (50 µg) were resolved by one-dimensional SDS-PAGE (12% acrylamide) under reducing conditions and electrophoretically transferred to polyvinylidene difluoride membranes (GE Amersham). Membranes were probed with primary antibodies against 14-3-3 mode 1 motif, GJA1, AKT, p (S473)-AKT, EIF4B, p (S422)-EIF4B, RPS6, p (S240/244)-RPS6, RPS6KB1, and p (T389)-RPS6KB1 (all diluted 1:1 000; using product no. 9606, 3512, 4691, 4060, 3592, 3591, 2317, 5364, 2708, and 9205, respectively; Cell Signaling); and p (T229)-RPS6KB1 (1:1 000 dilution; product ab5231; Abcam) or β-actin (ACTB; 1:10 000 dilution; product sc-47778; Santa Cruz Biotechnology) diluted in

Tris-buffered saline with 0.1% tween 20 containing 5% bovine serum albumin (Jackson ImmunoResearch Laboratories) or 5% dried milk. Following incubation with a horseradish peroxidase-conjugated secondary goat anti-rabbit antibody (1:10000 dilution; product W401B; Promega), the protein bands were visualized by chemiluminescence, using Immobilon Western chemiluminescent horseradish peroxidase substrate (Millipore).

Serum Testosterone Measurement

Blood samples were collected by cardiac puncture prior to euthanasia. Testosterone levels in the serum were determined by ELISA (IBL International). All assays were performed by the Ligand Assay and Analysis Core Laboratory of the University of Virginia.

Statistical Analyses

Student *t*-test was used for all comparisons between genotypes. Means were considered significantly different when *P* value was <0.05. All tests were carried out using Prism version 6.0d software (GraphPad Software, Inc).

RESULTS

Degeneration of the Seminiferous Tubules in *Mtor*^{flx/flx}; *Amhr2*^{cre/+} Mice

To investigate the role of mTOR signaling in the testis, a strategy was devised to inactivate *Mtor* in Sertoli cells. The *Amhr2*^{cre/+} strain, which has been shown to mainly drive Cre expression in Sertoli cells with no or minimal expression in adult Leydig cells [30–34], was crossed with an *Mtor*^{flx} strain that carries a *loxP* site upstream of the *Mtor* promoter region and a second *loxP* site in the intron preceding exon 6 [25]. To evaluate the efficiency of Cre-mediated recombination, Sertoli cells from 3-wk-old *Mtor*^{flx/flx}; *Amhr2*^{cre/+} and control *Mtor*^{flx/flx} animals were isolated and their genotype determined by PCR using genomic DNA. Analyses showed that approximately 50% of the floxed alleles were recombined in the cells from *Mtor*^{flx/flx}; *Amhr2*^{cre/+} mice (Fig. 1A). Consistent with this, RT-qPCR analysis showed a significant ~2-fold decrease in *Mtor* mRNA levels in the Sertoli cells from *Mtor*^{flx/flx}; *Amhr2*^{cre/+} mice (Fig. 1B). To confirm that Leydig cell function was not affected in *Mtor*^{flx/flx}; *Amhr2*^{cre/+} mice, serum testosterone levels were measured in 21-day-, 3-mo-, and 6-mo-old animals. No statistically significant differences between *Mtor*^{flx/flx}; *Amhr2*^{cre/+} and *Mtor*^{flx/flx} controls were observed at any age (Supplemental Table S2).

Mating trials were conducted as an initial screening for reproductive phenotypic anomalies in *Mtor*^{flx/flx}; *Amhr2*^{cre/+} mice. Four 6-wk-old mutant males and 4 age-matched male control *Mtor*^{flx/flx} mice were paired with 8-wk-old wild-type female mice for 6 mo. Whereas all females housed with *Mtor*^{flx/flx} males produced regular litters (~1/mo) throughout the trial, 3 of the 4 females housed with *Mtor*^{flx/flx}; *Amhr2*^{cre/+} males failed to produce a litter, and the fourth female produced a single litter. Gross morphological assessment of the testes from 21- to 55-day-old *Mtor*^{flx/flx}; *Amhr2*^{cre/+} mice showed them to be initially indistinguishable from those of their *Mtor*^{flx/flx} counterparts. However a progressive atrophy of the testes was detected in the *Mtor*^{flx/flx}; *Amhr2*^{cre/+} mice, starting at 3 mo of age, that was accompanied by a loss of germ cells (Fig. 2A). By 6 mo of age, testis weight in *Mtor*^{flx/flx}; *Amhr2*^{cre/+} animals was ~30% that of controls (Fig. 2B), indicating an important role for mTOR in the maintenance of spermatogenesis.

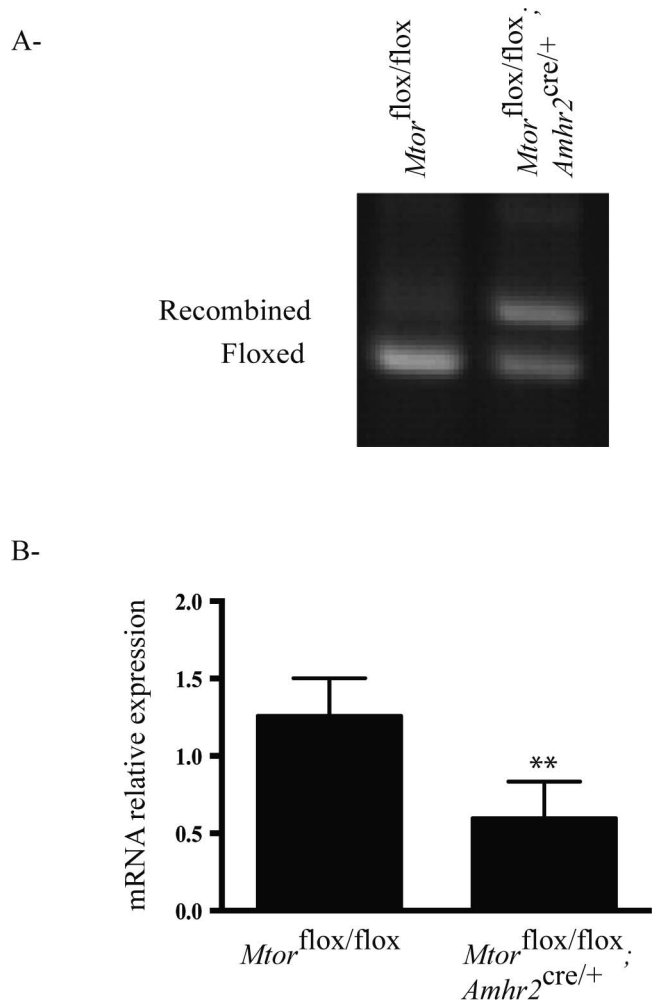


FIG. 1. *Mtor* knockdown efficiency in the *Mtor*^{flx/flx}; *Amhr2*^{cre/+} model. **A**) PCR genotype analyses of Sertoli cells isolated from 3-wk-old animals of the indicated genotypes. Samples were analyzed by electrophoresis using a 1% agarose gel containing ethidium bromide and photographed under UV illumination. Bands corresponding to the floxed and Cre-recombined alleles are indicated. **B**) RT-qPCR analysis of *Mtor* expression in the Sertoli cells of 3-wk-old mice of the indicated genotypes (*n* = 3 animals/genotype, performed in triplicate). All data were normalized to the housekeeping gene *Rpl19* and are expressed as mean (columns) ± SEM (error bars). **Significantly different from control (*P* < 0.01).

Spermatogenesis Is Abnormal in *Mtor*^{flx/flx}; *Amhr2*^{cre/+} Mice

To study the effects of *Mtor* deletion from Sertoli cells on germ cell development, we examined germ cell apoptosis by TUNEL assay. These analyses showed a precipitous increase in germ cell apoptosis in 3- and 6-mo-old *Mtor*^{flx/flx}; *Amhr2*^{cre/+} mice, indicating that the loss of *Mtor* hinders the survival of germ cells (Fig. 3). The timing of increased apoptosis roughly coincided with the onset of testicular atrophy and germ cell loss. Apoptosis of Sertoli cells was not observed at any age either by TUNEL or histopathologic analysis.

To identify the stages of germ cell development affected in *Mtor*^{flx/flx}; *Amhr2*^{cre/+} testes, histopathologic analysis was performed in 3-mo-old animals. The seminiferous tubules of *Mtor*^{flx/flx}; *Amhr2*^{cre/+} mice contained all 12 stages of spermatogenic cycle; however, an approximately 4-fold increase in numbers of degenerating pachytene spermatocytes

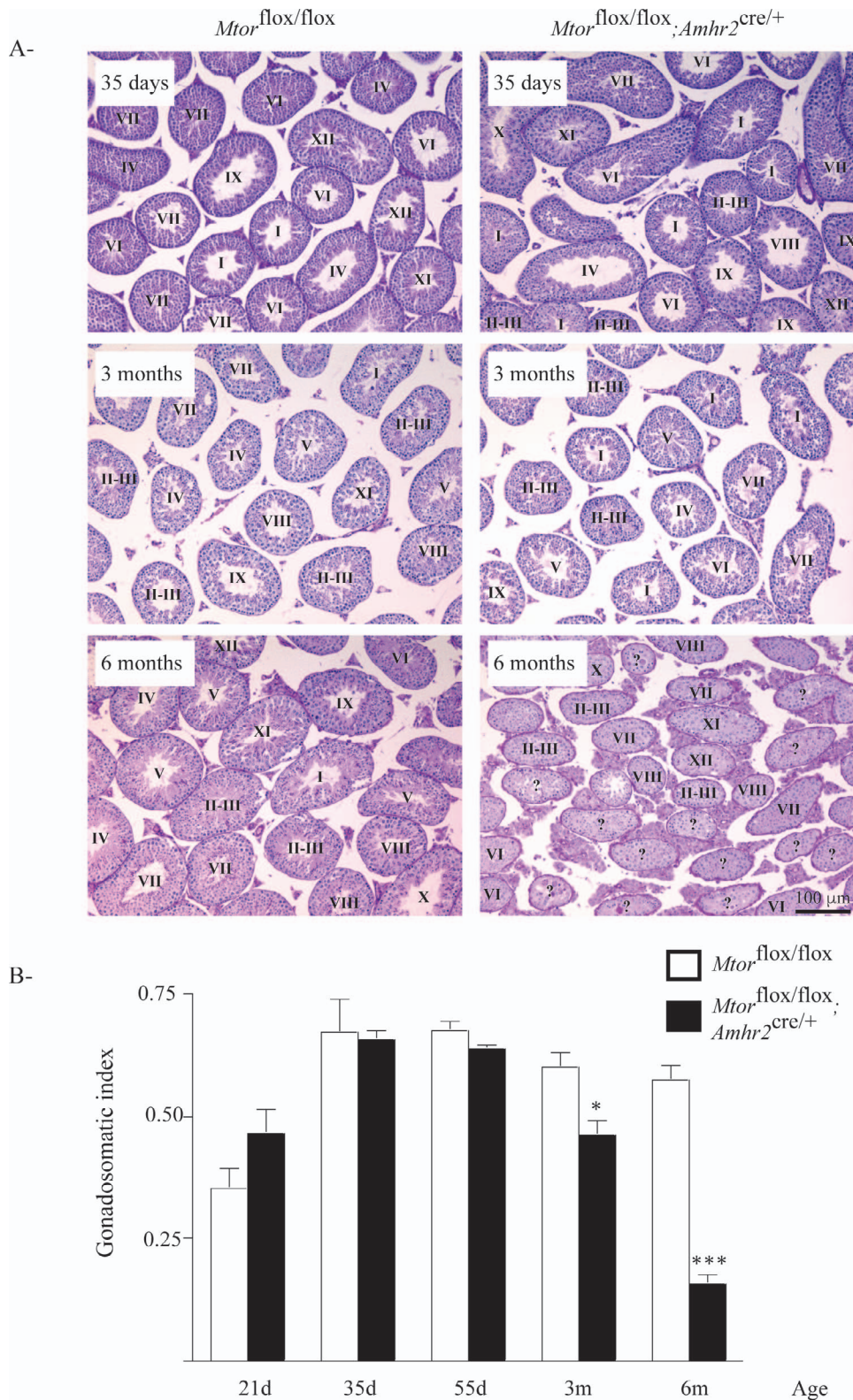


FIG. 2. Progressive degeneration of the seminiferous tubules in *Mtor*^{flox/flox};*Amhr2*^{cre/+} mice. **A**) Photomicrographs compare testicular histology of *Mtor*^{flox/flox};*Amhr2*^{cre/+} to that of *Mtor*^{flox/flox} controls at the indicated ages. Scale bar (lower right) is shown for all images; periodic acid-Schiff-hematoxylin stain. Stages of spermatogenic cycles are indicated for each tubule; stages could not be accurately determined for tubules marked with “?” due to loss of germ cells. **B**) Time course analysis of gonadosomatic index (testicular weight/corporeal weight) comparing *Mtor*^{flox/flox};*Amhr2*^{cre/+} to *Mtor*^{flox/flox} controls at the indicated ages. Sample numbers analyzed varied by age and genotype. Values for *Mtor*^{flox/flox};*Amhr2*^{cre/+} are 21d: n = 6; 35d: n = 4; 55d: n = 4; 3m: n = 8; 6m: n = 10; values for *Mtor*^{flox/flox} are 21d: n = 6; 35d: n = 3; 55d: n = 5; 3m: n = 5; 6m: n = 5. Data are expressed as means (columns) ± SEM (error bars). *Significant differences from controls (**P* < 0.05; ****P* < 0.001).

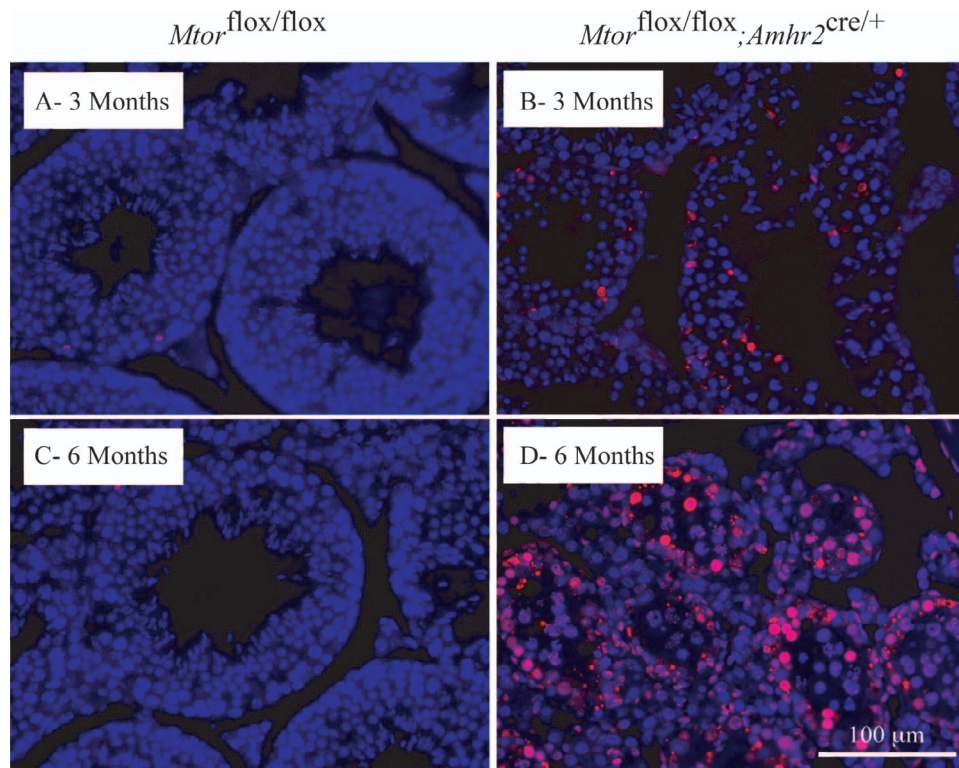


FIG. 3. Increased germ cell apoptosis in $Mtor^{flox/flox};Amhr2^{cre/+}$ testes. **A–D**) TUNEL stained samples (red) compare $Mtor^{flox/flox};Amhr2^{cre/+}$ mice to $Mtor^{flox/flox}$ controls at the indicated ages. DAPI (blue) was used as counterstain. Scale bar (lower right) is shown for all images.

and spermatids in stages VIII to X was observed relative to that in age-matched controls (Fig. 4, A and B). To further analyze germ cell development in $Mtor^{flox/flox};Amhr2^{cre/+}$ mice, the expression of molecular markers of specific stages was evaluated. No differences between expression of *Dmcl* (expressed prior to the pachytene spermatocyte stage) and that of *Sycp3* (expressed in spermatocytes up to and including the diplotene stage) were found between mutant and control animals. In contrast, testes from $Mtor^{flox/flox};Amhr2^{cre/+}$ mice showed significantly lower levels of expression of *Clgn* (expressed in pachytene spermatocytes), *Spert* (expressed in round spermatids) and *Dbil5* (expressed in elongating spermatids and mature spermatozoa) (Fig. 4C). Together, these results indicate that a defect in progression through the pachytene stage of spermatogenesis occurs in $Mtor^{flox/flox};Amhr2^{cre/+}$ mice.

We then evaluated the quantity and morphology of spermatozoa in the cauda epididymides of 3-mo-old and 6-mo-old $Mtor^{flox/flox};Amhr2^{cre/+}$ mice. Sperm counts in 3-mo-old $Mtor^{flox/flox};Amhr2^{cre/+}$ animals were not significantly reduced. On the other hand, a drastic decrease (98%) in spermatozoa present in epididymides was observed in 6-mo-old $Mtor^{flox/flox};Amhr2^{cre/+}$ mice (Fig. 5A). A significant increase in sperm abnormalities was also observed in both 3-mo-old (2.2-fold) and 6-mo-old (4.8-fold) $Mtor^{flox/flox};Amhr2^{cre/+}$ mice compared to age-matched controls (Fig. 5B). Most cells present in the epididymides of older animals were either elongated spermatids with large acrosomes or large round cells with two nuclei (symplasts), both indicative of premature release from the seminiferous epithelium (Fig. 5C). This premature release was also evident in the seminiferous tubules of $Mtor^{flox/flox};Amhr2^{cre/+}$ animals (Fig. 5D), was increased with age, and was associated with the disorganization of the seminiferous tubules and the loss of

polarity of some Sertoli cells (Fig. 5, E and F). These findings suggest that a gradual loss of attachments between Sertoli and germ cells occurs in the testes of $Mtor^{flox/flox};Amhr2^{cre/+}$ animals.

Altered Distribution of GJA1 in the Testes of $Mtor^{flox/flox};Amhr2^{cre/+}$ Mice

Because the loss of cohesion between Sertoli and germ cells was observed in the $Mtor^{flox/flox};Amhr2^{cre/+}$ testes and because both mTORC1 and mTORC2 complexes are thought to regulate BTB and junctional protein dynamics [20, 23], we next focused on potential effects of *Mtor* loss on the BTB and Sertoli–germ cell interaction dynamics. We first performed a biotin tracer assay in 3-mo-old animals to evaluate the integrity of the BTB. The biotin tracer was not able to pass through the BTB in either control or $Mtor^{flox/flox};Amhr2^{cre/+}$ mice, suggesting that the permeability of the BTB was not compromised in mutant animals (Supplemental Fig. S1, A and B, and Supplemental Materials and Methods). We next evaluated F-actin filaments and CTNNB1 (β -catenin), as both are components of the apical ectoplasmic specializations that normally prevent the sloughing of immature germ cells from the seminiferous epithelium [35]. Again, no differences were observed in the pattern of expression or distribution of F-actin (Supplemental Fig. S1, C and D, and Supplemental Materials and Methods) or CTNNB1 (Supplemental Fig. S1, E and F, and Supplemental Materials and Methods) within the seminiferous tubules between $Mtor^{flox/flox};Amhr2^{cre/+}$ mice and age-matched controls, suggesting that ectoplasmic specialization function was preserved in the mutant mice.

We next evaluated gap junction alpha-1 protein (GJA1; also known as connexin 43), a component of gap junctions, by immunohistochemistry. Contrary to the actin filaments and

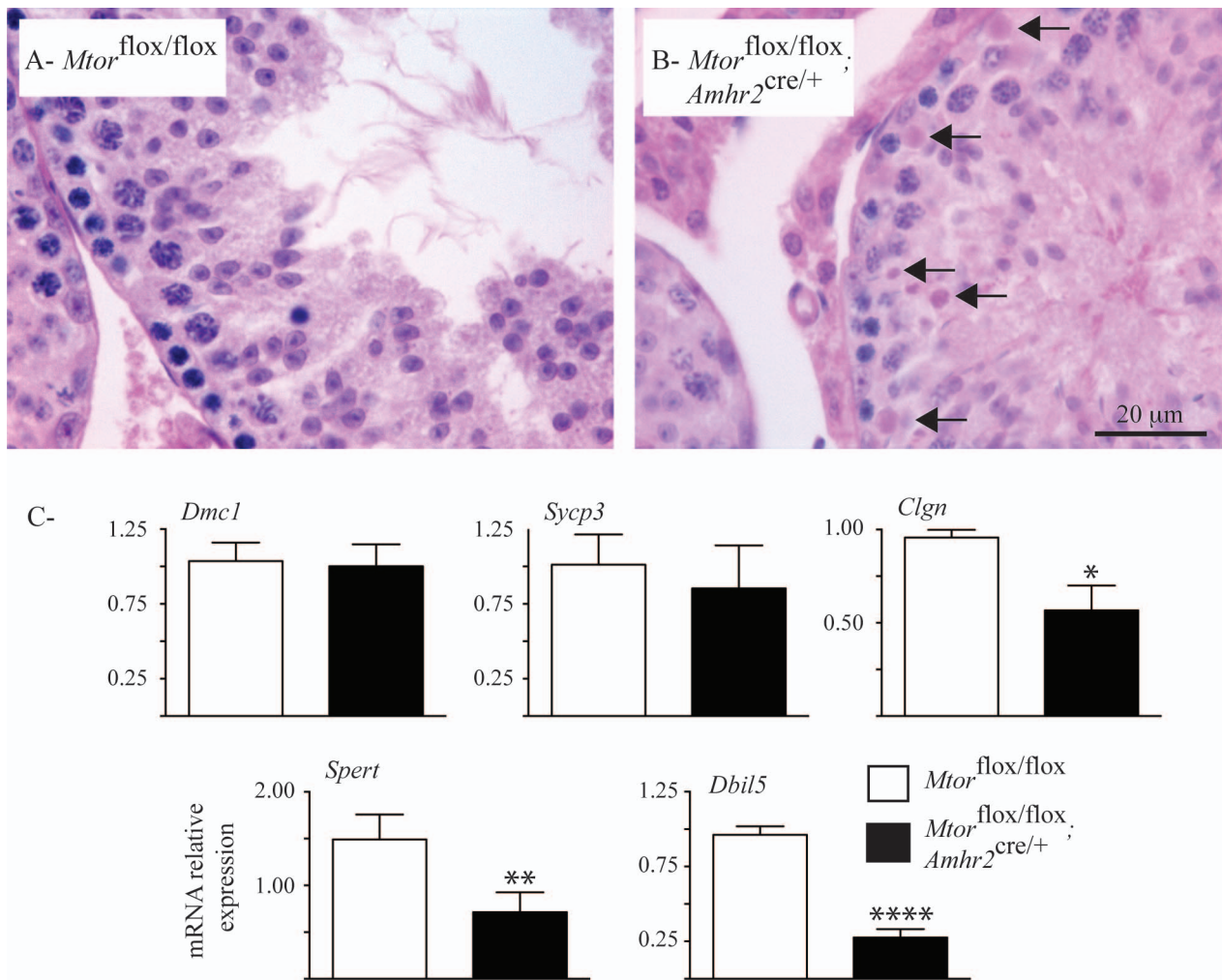


FIG. 4. Loss of pachytene spermatocytes and spermatids in the $Mtor^{flox/flox}; Amhr2^{cre/+}$ model. **A** and **B** Photomicrographs show increased numbers of degenerating spermatocytes (arrows) in stage IX tubules of 3-mo-old $Mtor^{flox/flox}; Amhr2^{cre/+}$ mice relative to those of age-matched $Mtor^{flox/flox}$ controls. Hematoxylin-eosin-phloxine-saffron stain. **C** RT-qPCR analysis is shown of the indicated spermatogenesis marker genes in testes from 3-mo-old $Mtor^{flox/flox}; Amhr2^{cre/+}$ and age-matched $Mtor^{flox/flox}$ mice ($n = 5$ animals/genotype). All data were normalized to the housekeeping gene *Rpl19* and are expressed as mean (columns) \pm SEM (error bars). *Significant differences from control (* $P < 0.05$; ** $P < 0.01$; **** $P < 0.0001$).

CTNBN1, GJA1 localization was altered in the testes of $Mtor^{flox/flox}; Amhr2^{cre/+}$ mice (Fig. 6, A and B). Whereas GJA1 localized mainly to expected locations of junctional complexes (i.e., mainly the BTB) in controls, a diffuse pattern of staining was observed in the Sertoli cells of $Mtor^{flox/flox}; Amhr2^{cre/+}$ mice. Because the phosphorylation of GJA1 at Ser373 leads to its internalization and downregulation at the cell surface [36], we then sought to determine the phosphorylation status of GJA1 in the testes of $Mtor^{flox/flox}; Amhr2^{cre/+}$ mice. This was done by GJA1 immunoprecipitation followed by immunoblotting using an antibody against the 14-3-3 mode-1 binding motif, which is created upon phosphorylation of GJA1 at Ser373 [37]. Binding motif 14-3-3 immunoreactivity (and hence GJA1 phosphorylation at Ser373) was markedly higher in the testes of $Mtor^{flox/flox}; Amhr2^{cre/+}$ mice than that in controls (Fig. 6C), suggesting a mechanism whereby the trafficking of GJA1 is altered in mutant Sertoli cells. Because GJA1 Ser373 is a target of AKT kinase [37, 38] and inhibition of mTORC1 has been shown to result in increased AKT activity in certain contexts [39, 40], we evaluated AKT expression and AKT phosphorylation at Ser473 in the testes of $Mtor^{flox/flox}; Amhr2^{cre/+}$ animals. Both total AKT and p (S473)-AKT expression were found to be upregulated in the testes of

$Mtor^{flox/flox}; Amhr2^{cre/+}$ mice (Fig. 6D). Together, these data suggest that the loss of germ cells in the $Mtor^{flox/flox}; Amhr2^{cre/+}$ model results, at least in part, from the upregulation of AKT, which interferes with gap junction dynamics by altering the trafficking of GJA1.

Phosphorylation of the mTORC1 Downstream Effectors RPS6K1 and EIF4B Is Downregulated in $Mtor^{flox/flox}; Amhr2^{cre/+}$ Testes

We next determined the effect of *Mtor* loss on the expression and phosphorylation of ribosomal protein S6 kinase 70 kDa polypeptide 1 (RPS6KB1) and eukaryotic initiation factor 4B (EIF4B), two key mTOR kinase targets and downstream effectors. Consistent with the loss of mTOR kinase activity, levels of phospho-EIF4B were markedly downregulated in the testes of $Mtor^{flox/flox}; Amhr2^{cre/+}$ mice (Fig. 7). Interestingly, total EIF4B levels were increased, suggesting a compensatory mechanism to offset the loss of phosphorylation. As for EIF4B, RPS6KB1 phosphorylation at (mTOR substrate) residue Thr389 was also markedly decreased, as was its phosphorylation at Thr229, a PDK1 phosphorylation site that becomes accessible following phos-

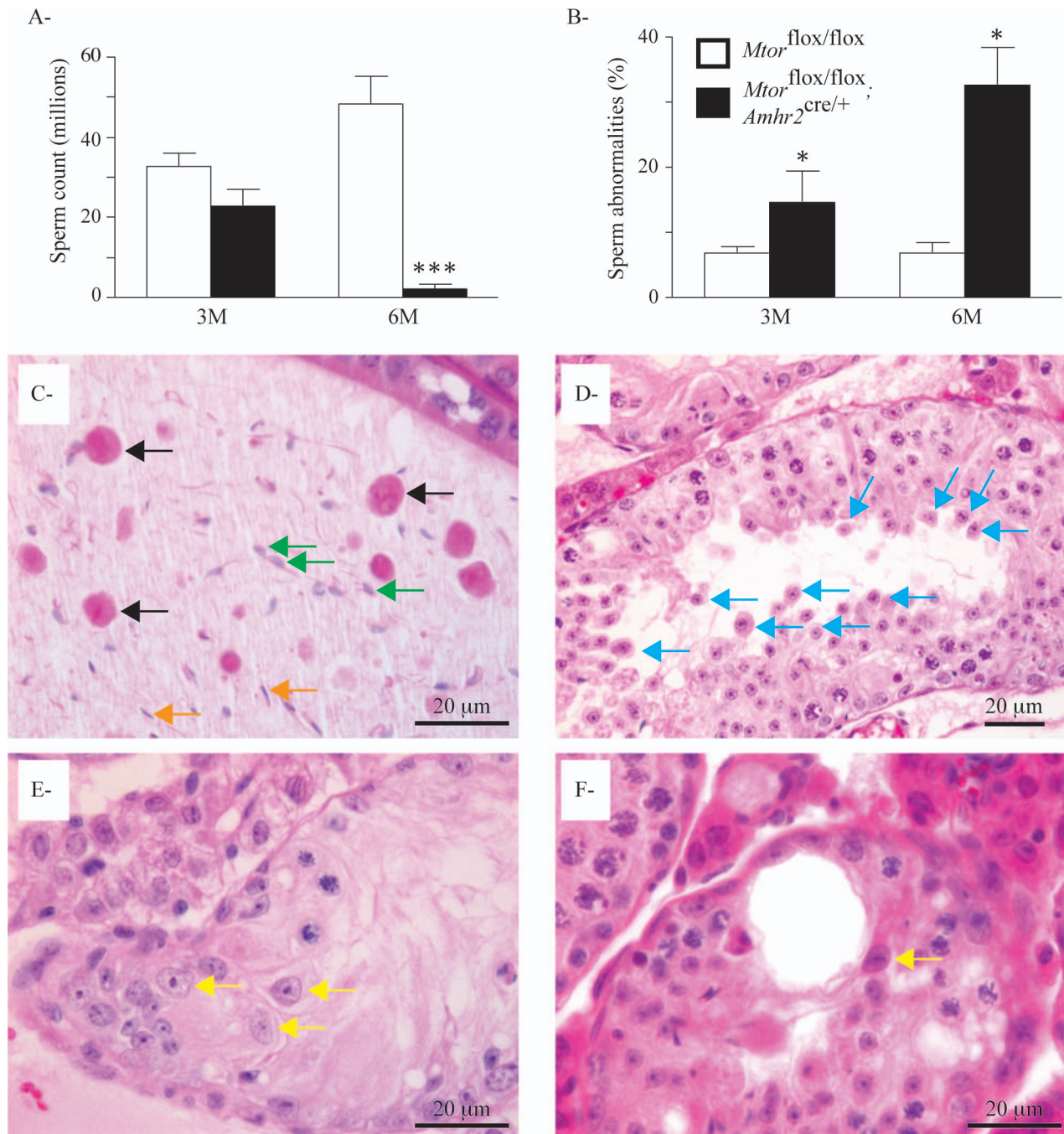


FIG. 5. Decreased sperm counts, increased abnormal spermatozoa, and premature release of germ cells in *Mtor*^{flox/flox}; *Amhr2*^{cre/+} mice. **A**) Cauda sperm counts in the epididymides of 3-mo-old and 6-mo-old *Mtor*^{flox/flox}; *Amhr2*^{cre/+} mice relative to those in age-matched *Mtor*^{flox/flox} controls. Sample numbers varied by age and genotype. Values for *Mtor*^{flox/flox}; *Amhr2*^{cre/+} were 3m: n = 6; 6m: n = 10; and values for *Mtor*^{flox/flox} were 3m: n = 5; and 6m: n = 4. Data are mean (columns) ± SEM (error bars). ***Significant differences from control ($P < 0.001$). **B**) Percentage of abnormal spermatozoa observed in the animals is described in **A**. Data are mean (columns) ± SEM (error bars), *Significant differences from control ($P < 0.05$). **C**) Photomicrograph of an epididymis of a 5-mo-old *Mtor*^{flox/flox}; *Amhr2*^{cre/+} mouse showing the presence of fused round spermatids (symplasts [black arrows]), elongated spermatids with large acrosomes (green arrows), and rare normal spermatozoa (orange arrows). **D**) Photomicrograph of a seminiferous tubule of a 5-mo-old *Mtor*^{flox/flox}; *Amhr2*^{cre/+} mouse showing premature release of spermatocytes (blue arrows). **E** and **F**) Photomicrographs of seminiferous tubules of 5-mo-old *Mtor*^{flox/flox}; *Amhr2*^{cre/+} mice showing ectopic localization of Sertoli cell nuclei and loss of cell polarity (yellow arrows). Hematoxylin-eosin-phloxine-saffron stain was used for all histologic sections.

phorylation at Thr389 [41–43] (Fig. 7). However, unlike EIF4B, total RPS6KB1 expression levels in the testes of *Mtor*^{flox/flox}; *Amhr2*^{cre/+} mice were comparable to those of controls. As loss of phosphorylation results in a loss of RPS6KB1 kinase activity, we evaluated the phosphorylation of the RPS6KB1 substrate RPS6. Unexpectedly, phosphorylation

of RPS6 at S235/236 was upregulated in the testes of the *Mtor*^{flox/flox}; *Amhr2*^{cre/+} animals (Fig. 7), suggesting compensatory mechanisms that offset the loss of RPS6KB1 activity. These results confirm that mTOR kinase activity is downregulated in the testes of *Mtor*^{flox/flox}; *Amhr2*^{cre/+} mice and suggest

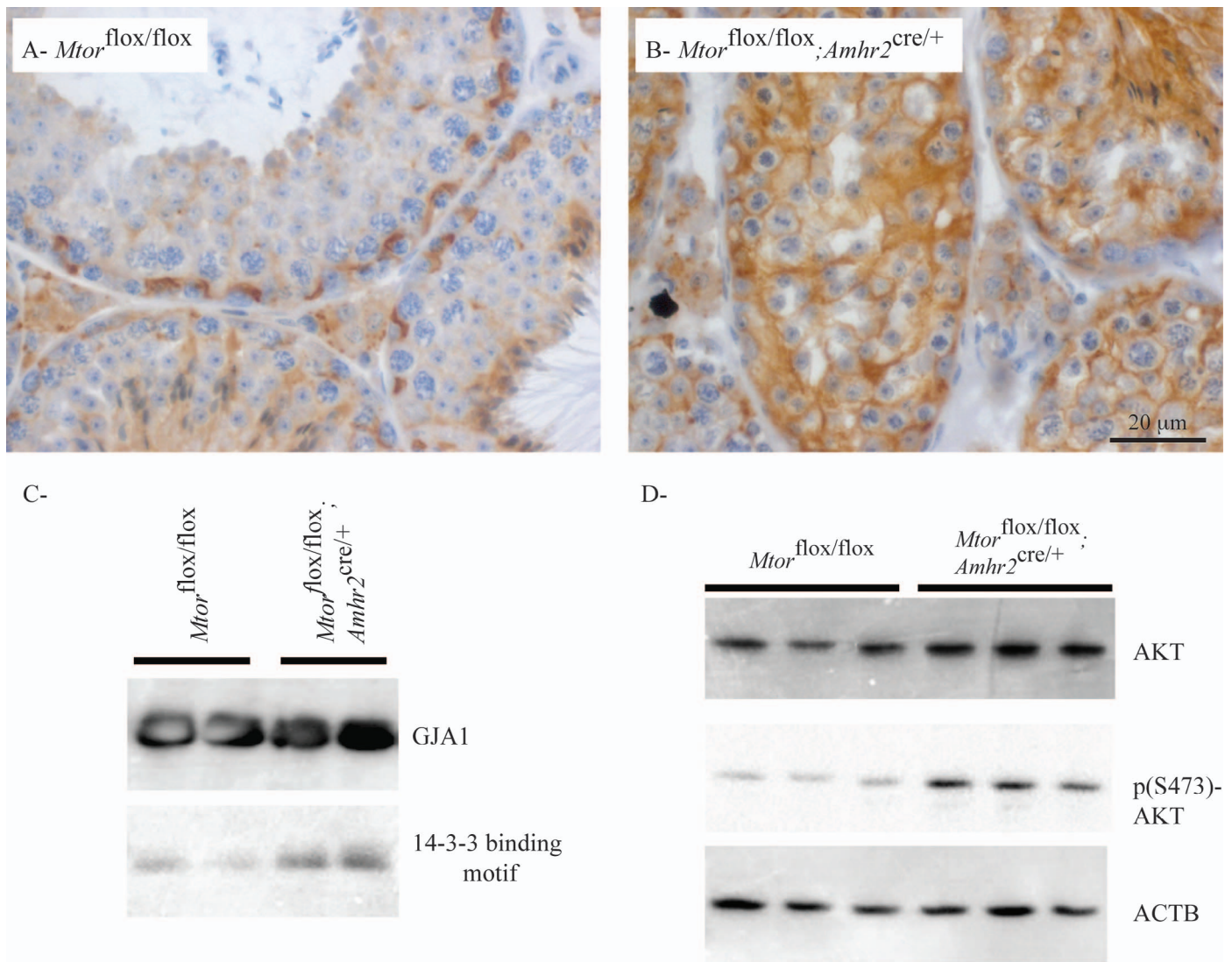


FIG. 6. Mislocalization of GJA1 in testes of $Mtor^{flox/flox};Amhr2^{cre/+}$ mice. **A** and **B**) Immunohistochemical analysis of GJA1 in testes from 3-mo-old $Mtor^{flox/flox};Amhr2^{cre/+}$ and $Mtor^{flox/flox}$ control mice. Scale bar in **B** is shown for both images. **C**) Immunoprecipitation of GJA1 followed by immunoblot analyses against GJA1 and the 14-3-3 mode 1 binding motif. Samples were total testicular protein extracts from 3-mo-old mice of the indicated genotypes (1 lane = 1 animal). Control immunoprecipitation reactions using IgG instead of the GJA1-specific antibody failed to immunoprecipitate 14-3-3 mode 1 binding motif-immunoreactive proteins (not shown). **D**) Immunoblot analysis of AKT and p(S473)-AKT in testes of 3-mo-old mice of the indicated genotypes is shown (1 lane = 1 animal). ACTB was used as the housekeeping control.

that the phenotypes observed in these testes are not due to a loss of RPS6 activation.

DISCUSSION

Although a few studies have reported the expression of mTOR signaling pathway components in Sertoli cells and evaluated potential mechanisms of action of mTOR downstream targets on BTB integrity [20–24], no study has directly evaluated the function of mTOR in Sertoli cells in vivo. Here, we report for the first time that the inactivation of *Mtor* in Sertoli cells results in the loss of their capacity to maintain spermatogenesis, which may be caused in part by the subcellular redistribution of GJA1. This provides the first in vivo functional evidence of the importance of mTOR signaling in the Sertoli cells of the postnatal testis.

During spermatogenesis, developing germ cells must traverse the seminiferous epithelium, a process that involves restructuring of the junctions between Sertoli cells, as well as

those between Sertoli and germ cells. The BTB represents a key junction between Sertoli cells and anatomically divides the seminiferous epithelium into the basal and the adluminal compartments. The BTB notably protects the adluminal compartment from the circulatory system, providing an immune-privileged microenvironment for the completion of meiosis. The BTB is composed of tight junctions, ectoplasmic specializations, desmosomes, and gap junctions [35]. Outside the BTB, additional ectoplasmic specializations exist that serve to anchor developing spermatids to Sertoli cells, along with desmosomes and gap junctions that anchor primary and secondary spermatocytes [35]. Our analyses of the testes of $Mtor^{flox/flox};Amhr2^{cre/+}$ mice showed a loss of polarity of Sertoli cells, degenerating pachytene spermatocytes and spermatids, and premature release of germ cells. All these findings are suggestive of altered restructuring and/or function of junctional complexes.

Several studies have suggested that both mTORC1 and mTORC2 could be involved in the restructuring of the BTB

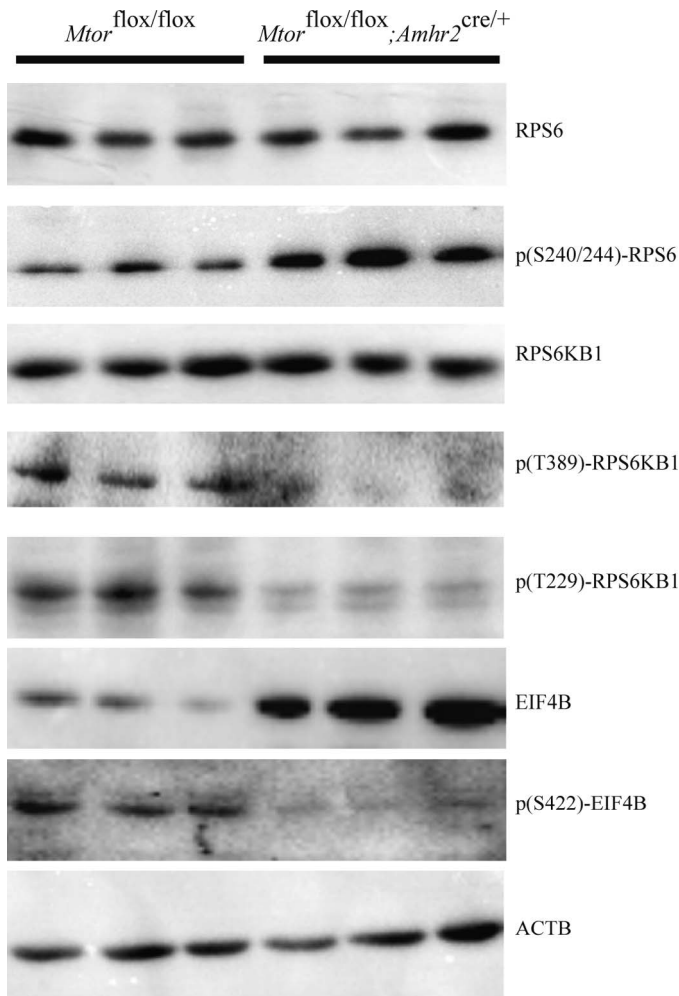


FIG. 7. Phosphorylation of the mTORC1 downstream effectors RPS6K1 and EIF4B (but not RPS6) is downregulated in testes of $Mtor^{flox/flox}; Amhr2^{cre/+}$ mice. Immunoblot analysis of the expression of the indicated downstream targets of mTOR in testes of 3-mo-old mice of the indicated genotypes (1 lane = 1 animal). ACTB was used as the housekeeping gene.

that occurs during spermatogenesis to permit germ cells to access the adluminal compartment [20–24]. In the current study, we were unable to find evidence of altered BTB function in the $Mtor^{flox/flox}; Amhr2^{cre/+}$ model. Likewise, we could not find obvious differences in the composition of ectoplasmic specializations. However, our investigation of gap junction dynamics revealed a striking redistribution of GJA1 within the Sertoli cells of $Mtor^{flox/flox}; Amhr2^{cre/+}$ mice, suggesting that altered function of gap junctions could be responsible for the spermatogenesis defects. Numerous studies have examined the effect of the loss of GJA1 in Sertoli cells by using the *SCCx43KO* conditional knockout model [44–49]. Those studies have shown that GJA1 expression in Sertoli cells is essential for normal testicular development, initiation of spermatogenesis, and fertility. Similar to the $Mtor^{flox/flox}; Amhr2^{cre/+}$ model, the BTB was found to be functional in *SCCx43KO* mice [45]. On the other hand, loss of germ cells in *SCCx43KO* mice occurs as early as 2 days of age [46], followed by an arrest of spermatogenesis at the level of the spermatogonia [44, 47]. This difference could be explained by the fact that *GJA1* was not knocked out in the $Mtor^{flox/flox}; Amhr2^{cre/+}$ model, and some level of gap junction functionality was therefore likely preserved, lessening the severity of the

phenotype. Also, whereas the $Amhr2^{cre}$ strain was used to drive Cre expression in the current study, the strain used to generate the *SCCx43KO* model was $Plekha5^{Tg} (AMH-cre)1^{Flor}$. Both the onset [31, 50, 51] and the efficiency of Cre-mediated recombination was therefore likely different between the models. Additional studies of GJA1 function in Sertoli cells have shown that replacement of GJA1 by gap junction beta-2 protein (GJB2) in transgenic mice impairs spermatogenesis, leading to the absence of germ cells beyond type I spermatocytes [52]. Furthermore, it was shown that an association between Sertoli cells and pachytene spermatocytes via GJA1 gap junctions is essential for the meiotic progression of spermatocytes in coculture [53]. Taken together, these studies and our present study suggest a crucial role of GJA1 in the late maturation of spermatocytes.

Post-translational modification has been shown to play an important role in gap junction channel assembly and function, and altered phosphorylation and trafficking of GJA1 are involved in the cause of several diseases [54–57]. We found an increased phosphorylation of GJA1 at Ser373 in the testes of $Mtor^{flox/flox}; Amhr2^{cre/+}$ mice, suggesting a mechanism underlying its mislocalization and potential altered function. The role of S373 phosphorylation in GJA1 trafficking was previously characterized in HaCaT cells and during acute cardiac ischemia. Phosphorylation of GJA1 on Ser373 was shown to activate a cascade leading to Ser368 and Ser255 phosphorylation and to the internalization of GJA1 [36]. Sequential phosphorylation of GJA1 starting with phosphorylation on Ser373 has also been implicated in the wound healing process, and leads to the increase of gap junction size, the inhibition of gap junction communication and the internalization of gap junctions from the plasma membrane [58, 59]. The early step of the internalization is possibly caused by the inability of GJA1 to bind to ZO-1, as S373 phosphorylation interferes with GJA1:ZO-1 interactions [38, 60–63]. Further studies will be required to determine if the interaction between GJA1, ZO-1 and other components of the gap junctions are altered in the $Mtor^{flox/flox}; Amhr2^{cre/+}$ model, as well as the extent to which gap junction communication is compromised.

As AKT can phosphorylate GJA1 at Ser373 [37, 38, 64], our observation that AKT expression and AKT phosphorylation on Ser473 are upregulated in the testes of $Mtor^{flox/flox}; Amhr2^{cre/+}$ mice provides a potential mechanism for explaining increased GJA1 phosphorylation. The phosphorylation of AKT on Ser473 has been mainly attributed to the rictor-mTORC2 complex [65–69] and is thought to be rictor-dependent [70]. However, as mTORC2 activity should be downregulated in the $Mtor^{flox/flox}; Amhr2^{cre/+}$ model, it would seem unlikely that mTORC2 is responsible for the increased phosphorylation of AKT observed in our study. A more likely explanation is that increased AKT activity is an indirect consequence of the loss of mTORC1 activity. Indeed, active RPS6KB1 regulates the IGF-1/insulin pathway by directly binding and phosphorylating IRS-1 [71–73], which promotes IRS-1 degradation and leads to a decrease in AKT activity. The downregulation of RPS6KB1 phosphorylation (and hence activity) that we observed in the testes of $Mtor^{flox/flox}; Amhr2^{cre/+}$ mice could therefore lead to the observed upregulation of AKT. Further experiments will be needed to determine if the IGF1/insulin signaling pathway is affected in the $Mtor^{flox/flox}; Amhr2^{cre/+}$ testes. Likewise, the paradoxical increase in the phosphorylation of RPS6 at S235/236 that we observed in the testes of the $Mtor^{flox/flox}; Amhr2^{cre/+}$ animals despite decreased RPS6KB1 activity remains to be explained. One possibility is that other RPS6 kinases, notably the four isoforms of the p90 ribosomal RPS6 kinase family of serine/threonine kinases (RSK), could be up-regulated in

response to the loss of RPS6KB1 activity. Our results therefore further demonstrate the complexity of the positive and negative feedback loops that regulate mTOR signaling.

In summary, this study reports, for the first time, a role for mTOR in Sertoli cell physiology in vivo. Inactivation of *Mtor* in Sertoli cells interferes with their capacity to support spermatogenesis and results in the premature release of germ cells, probably in part because of improper trafficking of GJA1. Additional studies will be required to define the specific roles of the mTORC1 and mTORC2 complexes in the observed phenotype.

ACKNOWLEDGMENT

We thank Dr. Robin Shaw (Cedars-Sinai Medical Center, Los Angeles) for advice regarding GJA1 immunoprecipitation and immunoblotting; Dr. Richard R. Behringer (University of Texas, Houston) for providing the *Amhr2^{Cre}* mice; and Dr. Sara C. Kozma (University of Cincinnati, Ohio) for providing the *Mtor^{flox}* mice.

REFERENCES

- Laplante M, Sabatini DM. mTOR signaling in growth control and disease. *Cell* 2012; 149:274–293.
- Appenzeller-Herzog C, Hall MN. Bidirectional crosstalk between endoplasmic reticulum stress and mTOR signaling. *Trends Cell Biol* 2012; 22:274–282.
- Chi H. Regulation and function of mTOR signalling in T cell fate decisions. *Nat Rev Immunol* 2012; 12:325–338.
- Nair S, Ren J. Autophagy and cardiovascular aging: lesson learned from rapamycin. *Cell Cycle* 2012; 11:2092–2099.
- Dazert E, Hall MN. mTOR signaling in disease. *Curr Opin Cell Biol* 2011; 23:744–755.
- Chen Y, Zhang Z, Lin Y, Lin H, Li M, Nie P, Chen L, Qiu J, Lu Y, Chen L, Xu B, Lin W, et al. Long-term impact of immunosuppressants at therapeutic doses on male reproductive system in unilateral nephrectomized rats: a comparative study. *Biomed Res Int* 2013; 2013:690382.
- Deutsch MA, Kaczmarek I, Huber S, Schmauss D, Beiras-Fernandez A, Schmoedel M, Ochsenkuehn R, Meiser B, Mueller-Hoecker J, Reichart B. Sirolimus-associated infertility: case report and literature review of possible mechanisms. *Am J Transplant* 2007; 7:2414–2421.
- Bererhi L, Flamant M, Martinez F, Karras A, Thervet E, Legendre C. Rapamycin-induced oligospermia. *Transplantation* 2003; 76:885–886.
- Fritsche L, Budde K, Dragun D, Einecke G, Diekmann F, Neumayer HH. Testosterone concentrations and sirolimus in male renal transplant patients. *Am J Transplant* 2004; 4:130–131.
- Huyghe E, Zairi A, Nohra J, Kamar N, Plante P, Rostaing L. Gonadal impact of target of rapamycin inhibitors (sirolimus and everolimus) in male patients: an overview. *Transpl Int* 2007; 20:305–311.
- Kaczmarek I, Groetzer J, Adamidis I, Landwehr P, Mueller M, Vogeser M, Gerstorfer M, Uberfuhr P, Meiser B, Reichart B. Sirolimus impairs gonadal function in heart transplant recipients. *Am J Transplant* 2004; 4: 1084–1088.
- Lee S, Coco M, Greenstein SM, Schechner RS, Tellis VA, Glicklich DG. The effect of sirolimus on sex hormone levels of male renal transplant recipients. *Clin Transplant* 2005; 19:162–167.
- Hobbs RM, Seandel M, Falcatori I, Rafii S, Pandolfi PP. Plzf regulates germline progenitor self-renewal by opposing mTORC1. *Cell* 2010; 142: 468–479.
- Busada JT, Chappell VA, Niedenberger BA, Kaye EP, Keiper BD, Hogarth CA, Geyer CB. Retinoic acid regulates Kit translation during spermatogonial differentiation in the mouse. *Dev Biol* 2015; 397:140–149.
- Busada JT, Niedenberger BA, Velte EK, Keiper BD, Geyer CB. Mammalian target of rapamycin complex 1 (mTORC1) is required for mouse spermatogonial differentiation in vivo. *Dev Biol* 2015; 407: 90–102.
- Hobbs RM, La HM, Makela JA, Kobayashi T, Noda T, Pandolfi PP. Distinct germline progenitor subsets defined through Tsc2-mTORC1 signaling. *EMBO Rep* 2015; 16:467–480.
- Musnier A, Heitzler D, Boulo T, Tesseraud S, Durand G, Lecureuil C, Guillou H, Poupon A, Reiter E, Crepieux P. Developmental regulation of p70 S6 kinase by a G protein-coupled receptor dynamically modeled in primary cells. *Cell Mol Life Sci* 2009; 66:3487–3503.
- Riera MF, Regueira M, Galardo MN, Pellizzari EH, Meroni SB, Cigorraga SB. Signal transduction pathways in FSH regulation of rat Sertoli cell proliferation. *Am J Physiol Endocrinol Metab* 2012; 302:E914–923.
- Jesus TT, Oliveira PF, Silva J, Barros A, Ferreira R, Sousa M, Cheng CY, Silva BM, Alves MG. Mammalian target of rapamycin controls glucose consumption and redox balance in human Sertoli cells. *Fertil Steril* 2016; 105:825–833. e823.
- Mok KW, Mruk DD, Silvestrini B, Cheng CY. rpS6 Regulates blood-testis barrier dynamics by affecting F-actin organization and protein recruitment. *Endocrinology* 2012; 153:5036–5048.
- Mok KW, Mruk DD, Cheng CY. rpS6 regulates blood-testis barrier dynamics through Akt-mediated effects on MMP-9. *J Cell Sci* 2014; 127: 4870–4882.
- Mok KW, Chen H, Lee WM, Cheng CY. rpS6 regulates blood-testis barrier dynamics through Arp3-mediated actin microfilament organization in rat Sertoli cells. An in vitro study. *Endocrinology* 2015; 156: 1900–1913.
- Mok KW, Mruk DD, Lee WM, Cheng CY. Rictor/mTORC2 regulates blood-testis barrier dynamics via its effects on gap junction communications and actin filament network. *FASEB J* 2013; 27:1137–1152.
- Dong H, Chen Z, Wang C, Xiong Z, Zhao W, Jia C, Lin J, Lin Y, Yuan W, Zhao AZ, Bai X. Rictor regulates spermatogenesis by controlling Sertoli cell cytoskeletal organization and cell polarity in the mouse testis. *Endocrinology* 2015; 156:4244–4256.
- Risson V, Mazelin L, Roceri M, Sanchez H, Moncollin V, Comeloup C, Richard-Bulteau H, Vignaud A, Baas D, Defour A, Freyssenet D, Tanti JF, et al. Muscle inactivation of mTOR causes metabolic and dystrophin defects leading to severe myopathy. *J Cell Biol* 2009; 187:859–874.
- Jorgez CJ, Klysik M, Jamin SP, Behringer RR, Matzuk MM. Granulosa cell-specific inactivation of follistatin causes female fertility defects. *Mol Endocrinol* 2004; 18:953–967.
- Boyer A, Yeh JR, Zhang X, Paquet M, Gaudin A, Nagano MC, Boerboom D. CTNNB1 signaling in Sertoli cells downregulates spermatogonial stem cell activity via WNT4. *PLoS One* 2012; 7:e29764.
- Wang Y. Epididymal sperm count. *Curr Protoc Toxicol* 2003; 16: 16.6.1–16.6.5.
- Russell LDER, Hikim APS, Clegg ED. *Histological and Histopathological Evaluation of the Testis*. Clearwater, FL: Cache River Press; 1990; 62–104.
- Boyer A, Hermo L, Paquet M, Robaire B, Boerboom D. Seminiferous tubule degeneration and infertility in mice with sustained activation of WNT/CTNNB1 signaling in Sertoli cells. *Biol Reprod* 2008; 79:475–485.
- Tanwar PS, Kaneko-Tarui T, Zhang L, Rani P, Taketo MM, Teixeira J. Constitutive WNT/beta-catenin signaling in murine Sertoli cells disrupts their differentiation and ability to support spermatogenesis. *Biol Reprod* 2010; 82:422–432.
- Tanwar PS, Kaneko-Tarui T, Zhang L, Teixeira JM. Altered LKB1/AMPK/TSC1/TSC2/mTOR signaling causes disruption of Sertoli cell polarity and spermatogenesis. *Hum Mol Genet* 2012; 21:4394–4405.
- Kato T, Esaki M, Matsuzawa A, Ikeda Y. NR5A1 is required for functional maturation of Sertoli cells during postnatal development. *Reproduction* 2012; 143:663–672.
- Kyronlahti A, Euler R, Bielinska M, Schoeller EL, Moley KH, Toppari J, Heikinheimo M, Wilson DB. GATA4 regulates Sertoli cell function and fertility in adult male mice. *Mol Cell Endocrinol* 2011; 333:85–95.
- Mruk DD, Cheng CY. The mammalian blood-testis barrier: its biology and regulation. *Endocr Rev* 2015; 36:564–591.
- Smyth JW, Zhang SS, Sanchez JM, Lamouille S, Vogan JM, Hesketh GG, Hong T, Tomaselli GF, Shaw RMA. 14-3-3 mode-1 binding motif initiates gap junction internalization during acute cardiac ischemia. *Traffic* 2014; 15:684–699.
- Park DJ, Freitas TA, Wallick CJ, Guyette CV, Warn-Cramer BJ. Molecular dynamics and in vitro analysis of connexin43: a new 14-3-3 mode-1 interacting protein. *Protein Sci* 2006; 15:2344–2355.
- Dunn CA, Lampe PD. Injury-triggered Akt phosphorylation of Cx43: a ZO-1-driven molecular switch that regulates gap junction size. *J Cell Sci* 2014; 127:455–464.
- O'Reilly KE, Rojo F, She QB, Solit D, Mills GB, Smith D, Lane H, Hofmann F, Hicklin DJ, Ludwig DL, Baselga J, Rosen N. mTOR inhibition induces upstream receptor tyrosine kinase signaling and activates Akt. *Cancer Res* 2006; 66:1500–1508.
- Sun SY, Rosenberg LM, Wang X, Zhou Z, Yue P, Fu H, Khuri FR. Activation of Akt and eIF4E survival pathways by rapamycin-mediated mammalian target of rapamycin inhibition. *Cancer Res* 2005; 65: 7052–7058.
- Kim DH, Sarbassov DD, Ali SM, King JE, Latek RR, Erdjument-Bromage H, Tempst P, Sabatini DM. mTOR interacts with raptor to form a nutrient-

- sensitive complex that signals to the cell growth machinery. *Cell* 2002; 110:163–175.
42. Holz MK, Blenis J. Identification of S6 kinase 1 as a novel mammalian target of rapamycin (mTOR)-phosphorylating kinase. *J Biol Chem* 2005; 280:26089–26093.
 43. Alessi DR, Kozlowski MT, Weng QP, Morrice N, Avruch J. 3-Phosphoinositide-dependent protein kinase 1 (PDK1) phosphorylates and activates the p70 S6 kinase in vivo and in vitro. *Curr Biol* 1998; 8: 69–81.
 44. Brehm R, Zeiler M, Ruttinger C, Herde K, Kibschull M, Winterhager E, Willecke K, Guillou F, Lecureuil C, Steger K, Konrad L, Biermann K, et al. A Sertoli cell-specific knockout of connexin43 prevents initiation of spermatogenesis. *Am J Pathol* 2007; 171:19–31.
 45. Carette D, Weider K, Gilleron J, Giese S, Dompierre J, Bergmann M, Brehm R, Denizot JP, Segretain D, Pointis G. Major involvement of connexin 43 in seminiferous epithelial junction dynamics and male fertility. *Dev Biol* 2010; 346:54–67.
 46. Giese S, Hossain H, Markmann M, Chakraborty T, Tchatalbachev S, Guillou F, Bergmann M, Failing K, Weider K, Brehm R. Sertoli-cell-specific knockout of connexin 43 leads to multiple alterations in testicular gene expression in prepubertal mice. *Dis Model Mech* 2012; 5:895–913.
 47. Sridharan S, Simon L, Meling DD, Cyr DG, Gutstein DE, Fishman GI, Guillou F, Cooke PS. Proliferation of adult Sertoli cells following conditional knockout of the Gap junctional protein GJA1 (connexin 43) in mice. *Biol Reprod* 2007; 76:804–812.
 48. Gerber J, Weider K, Hambruch N, Brehm R. Loss of connexin43 (Cx43) in Sertoli cells leads to spatio-temporal alterations in occludin expression. *Histol Histopathol* 2014; 29:935–948.
 49. Gerber J, Heinrich J, Brehm R. Blood-testis barrier and Sertoli cell function: lessons from SCCx43KO mice. *Reproduction* 2016; 151: R15–r27.
 50. Arango NA, Kobayashi A, Wang Y, Jamin SP, Lee HH, Orvis GD, Behringer RR. A mesenchymal perspective of Müllerian duct differentiation and regression in *Amhr2-lacZ* mice. *Mol Reprod Dev* 2008; 75: 1154–1162.
 51. Lecureuil C, Fontaine I, Crepieux P, Guillou F. Sertoli and granulosa cell-specific Cre recombinase activity in transgenic mice. *Genesis* 2002; 33: 114–118.
 52. Winterhager E, Pielensticker N, Freyer J, Ghanem A, Schrickel JW, Kim JS, Behr R, Grummer R, Maass K, Urschel S, Lewalter T, Tiemann K, et al. Replacement of connexin43 by connexin26 in transgenic mice leads to dysfunctional reproductive organs and slowed ventricular conduction in the heart. *BMC Dev Biol* 2007; 7:26.
 53. Godet M, Sabido O, Gilleron J, Durand P. Meiotic progression of rat spermatocytes requires mitogen-activated protein kinases of Sertoli cells and close contacts between the germ cells and the Sertoli cells. *Dev Biol* 2008; 315:173–188.
 54. Beardslee MA, Lerner DL, Tadros PN, Laing JG, Beyer EC, Yamada KA, Kleber AG, Schuessler RB, Saffitz JE. Dephosphorylation and intracellular redistribution of ventricular connexin43 during electrical uncoupling induced by ischemia. *Circ Res* 2000; 87:656–662.
 55. Hesketh GG, Shah MH, Halperin VL, Cooke CA, Akar FG, Yen TE, Kass DA, Machamer CE, Van Eyk JE, Tomaselli GF. Ultrastructure and regulation of lateralized connexin43 in the failing heart. *Circ Res* 2010; 106:1153–1163.
 56. Hoos MD, Richardson BM, Foster MW, Everhart A, Thompson JW, Moseley MA, Colton CA. Longitudinal study of differential protein expression in an Alzheimer's mouse model lacking inducible nitric oxide synthase. *J Proteome Res* 2013; 12:4462–4477.
 57. Wang Y, Wu Z, Liu X, Fu Q. Gastrodin ameliorates Parkinson's disease by downregulating connexin 43. *Mol Med Rep* 2013; 8:585–590.
 58. Qiu C, Coutinho P, Frank S, Franke S, Law LY, Martin P, Green CR, Becker DL. Targeting connexin43 expression accelerates the rate of wound repair. *Curr Biol* 2003; 13:1697–1703.
 59. Richards TS, Dunn CA, Carter WG, Usui ML, Olerud JE, Lampe PD. Protein kinase C spatially and temporally regulates gap junctional communication during human wound repair via phosphorylation of connexin43 on serine368. *J Cell Biol* 2004; 167:555–562.
 60. Chen J, Pan L, Wei Z, Zhao Y, Zhang M. Domain-swapped dimerization of ZO-1 PDZ2 generates specific and regulatory connexin43-binding sites. *EMBO J* 2008; 27:2113–2123.
 61. Hunter AW, Barker RJ, Zhu C, Gourdie RG. Zonula occludens-1 alters connexin43 gap junction size and organization by influencing channel accretion. *Mol Biol Cell* 2005; 16:5686–5698.
 62. O'Quinn MP, Palatinus JA, Harris BS, Hewett KW, Gourdie RG. A peptide mimetic of the connexin43 carboxyl terminus reduces gap junction remodeling and induced arrhythmia following ventricular injury. *Circ Res* 2011; 108:704–715.
 63. Palatinus JA, O'Quinn MP, Barker RJ, Harris BS, Jourdan J, Gourdie RG. ZO-1 determines adherens and gap junction localization at intercalated disks. *Am J Physiol Heart Circ Physiol* 2011; 300:H583–594.
 64. Batra N, Riquelme MA, Burra S, Kar R, Gu S, Jiang JX. Direct regulation of osteocytic connexin 43 hemichannels through AKT kinase activated by mechanical stimulation. *J Biol Chem* 2014; 289:10582–10591.
 65. Sarbassov DD, Guertin DA, Ali SM, Sabatini DM. Phosphorylation and regulation of Akt/PKB by the rictor-mTOR complex. *Science* 2005; 307: 1098–1101.
 66. Bhaskar PT, Hay N. The two TORCs and Akt. *Dev Cell* 2007; 12: 487–502.
 67. Bhaskar PT, Nogueira V, Patra KC, Jeon SM, Park Y, Robey RB, Hay N. mTORC1 hyperactivity inhibits serum deprivation-induced apoptosis via increased hexokinase II and GLUT1 expression, sustained Mcl-1 expression, and glycogen synthase kinase 3beta inhibition. *Mol Cell Biol* 2009; 29:5136–5147.
 68. Chiang GG, Abraham RT. Targeting the mTOR signaling network in cancer. *Trends Mol Med* 2007; 13:433–442.
 69. Tenkerian C, Krishnamoorthy J, Mounir Z, Kazimierczak U, Khoutorsky A, Staschke KA, Kristof AS, Wang S, Hatzoglou M, Koromilas AE. mTORC2 balances Akt activation and eIF2alpha serine 51 phosphorylation to promote survival under stress. *Mol Cancer Res* 2015; 13: 1377–1388.
 70. Breuleux M, Klopfenstein M, Stephan C, Doughty CA, Barys L, Maira SM, Kwiatkowski D, Lane HA. Increased AKT S473 phosphorylation after mTORC1 inhibition is rictor dependent and does not predict tumor cell response to PI3K/mTOR inhibition. *Mol Cancer Ther* 2009; 8: 742–753.
 71. Harrington LS, Findlay GM, Gray A, Tolkacheva T, Wigfield S, Rebholz H, Barnett J, Leslie NR, Cheng S, Shepherd PR, Gout I, Downes CP, et al. The TSC1-2 tumor suppressor controls insulin-PI3K signaling via regulation of IRS proteins. *J Cell Biol* 2004; 166:213–223.
 72. Zhang J, Gao Z, Yin J, Quon MJ, Ye J. S6K directly phosphorylates IRS-1 on Ser-270 to promote insulin resistance in response to TNF-(alpha) signaling through IKK2. *J Biol Chem* 2008; 283:35375–35382.
 73. Tremblay F, Brule S, Hee Um S, Li Y, Masuda K, Roden M, Sun XJ, Krebs M, Polakiewicz RD, Thomas G, Marette A. Identification of IRS-1 Ser-1101 as a target of S6K1 in nutrient- and obesity-induced insulin resistance. *Proc Natl Acad Sci U S A* 2007; 104:14056–14061.